ACS Catalysis

pubs.acs.org/acscatalysis Letter

Hydroarylation of Activated Alkenes Enabled by Proton-Coupled Electron Transfer

Zhaosheng Liu, Shuai Zhong, Xiaochen Ji,* Guo-Jun Deng, and Huawen Huang*

Cite This: *ACS Catal.* 2021, 11, 4422–4429 Read Online

ACCESS | Metrics & More | Article Recommendations | Supporting Information

ABSTRACT: Hydroarylation of alkenes has been demonstrated to be an atom-economic approach to access functionalized arenes from easily accessible raw materials. Herein, we report a visible light-induced photocatalytic system that enables intramolecular hydroarylation of N-arylacrylamides with high 5-exo-trig selectivity through robust proton-coupled electron transfer (PCET). This mild hydroarylation protocol provides a straightforward entry to structurally valuable oxindoles and complements previously established 6-endo-trig cyclization by photochemical triplet energy transfer (TET).

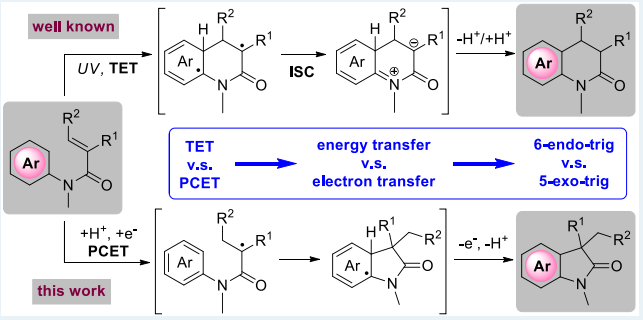

KEYWORDS: *hydroarylation, proton-coupled electron transfer, photocatalysis, visible light driven, cyclization*

Hydrofunctionalization of alkenes is one of the most important transformations in synthetic chemistry that leads to reliable approaches for viable formation of C(sp^3)−C and C(sp^3)−heteroatom bonds.[1] Specifically, hydroarylation has been traditionally achieved by the Friedel−Crafts process with proton transfer and transition metal-mediated reductive Heck-type couplings (RHC; Figure 1a).[2] While in the former method the formation of high energy carbocations requires strong acidic conditions and restricts the substrates to both electron-rich alkenes and arenes, the latter highly depends on the use of noble metal catalysts and organometallic reagents or their prefunctionalized precursors. In the past few decades, radical addition couplings of alkenes by metal-hydride hydrogen-atom transfer (MHHAT) have been found practical applications in hydroarylation (Figure 1b),[1a] which are typically initiated by cheap and low-toxicity metals such as Fe, Mn, Co, etc.[3] More importantly, such reactions proceed under mild conditions, and thereby chemoselectivities are generally well controlled with broader functional group tolerance. Remarkably, Gansäuer and co-workers have demonstrated titanocene-catalyzed regiodivergent radical hydroarylations of epoxides, with even ready achievement of enantioselective catalysis.[4]

Photochemical transformation provides a powerful and versatile platform for molecule synthesis.[5] With light stimulation, triplet energy transfer (TET) from an appropriate sensitizer forms a highly activated triplet state (T1) of alkenes that initiates an alternative approach for hydroarylation of alkenes (Figure 1c).[6] Within this field, photoinduced 6π-electrocyclization[7] and [2 + 2] cycloaddition[8] have been well established especially for intramolecular alkene functionaliza-

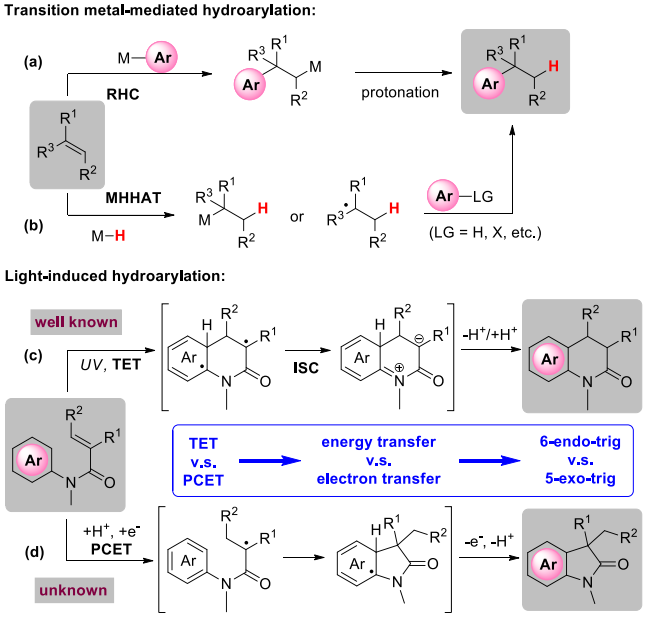

Figure 1. Hydroarylation methods.

Received: February 10, 2021
Revised: March 22, 2021
Published: March 26, 2021

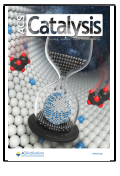

https://doi.org/10.1021/acscatal.1c00649
ACS Catal. 2021, 11, 4422–4429

tion and hydroarylation. Recently, Smith et al. exploited the interrupted [2 + 2] cycloaddition strategy and ingeniously designed *N*-acryloyl indoles and related heterocycles,[9] which lead to high yielding heterocycle functionalization/γ-lactam formation with the aid of sustainable visible light. During the preparation of this paper, Che and co-workers reported photoinduced hydroarylation and cyclization of alkenes with a luminescent platinum(II) complex.[10] Hence, the facile formation of structurally diverse 3,4-dihydroquinolinones was achieved from N-arylacrylamides, again, with 6-endo-trig cyclization selectivity via 6π-electrocyclization.

On the other hand, photodriven proton-coupled electron transfer (PCET)[11] has been demonstrated to be capable of overcoming the activation barrier under mild conditions in radial couplings of unsaturated compounds including imines and carbonyls.[12] However, hydroarylation of alkenes via the PCET process has rarely been exploited.[13] In view of the ready formation and stability of the α carbon radical of N-arylamides through radical addition to N-arylacrylamides,[14] we envision that the reductive PCET of N-arylacrylamides could occur to form the same radical species, with further 5-exo-trig cyclization followed by single-electron oxidation and deprotonation to access pharmaceutically significant oxindoles (Figure 1d). Although the same transformation has been realized by hydrometalation under thermal conditions,[3b,c] the milder photocatalysis with 5-exo-trig selectivity of N-arylacrylamides remains challenging. Hence, to enable such a redox-neutral hydroarylation of alkenes, an appropriate photocatalyst with both strong reductive and oxidative potentials is required. Moreover, the key challenge to realize it should be to find a novel photocatalytic system in which the chemoselectivity can be turned from 6-endo-trig cyclization selectivity via TET over 5-exo-trig selectivity via PCET.

The resultant oxindole skeleton is an important motif found in numerous drugs and naturally occurring compounds. Although transition-metal-catalyzed processes have been utilized to enable direct formation of this structure from N-arylacrylamides,[15] to our knowledge, there are no examples using mild visible-light-mediated PCET. To exploit the feasibility of this method, we selected *N*-methyl-*N*-phenylmethacrylamide (**1a**) as the model substrate to test its reactivity under irradiation with 35 W blue LED light (Table 1). Our systematic optimization of reaction conditions reveals that the combinational use of $Ir(dF(CF_3)ppy)_2(dtbpy)]PF_6$ as the catalyst, TfOH as the proton source, and LiBr as the electron mediator is the key to success in the intramolecular 5-exo-trig hydroarylation. The results from the screening of a range of photocatalysts have verified our speculation that the photocatalysts with both strong reductive and oxidative potentials enable the 5-exo-trig cyclization, where $Ir(dF(CF_3)ppy)_2(dtbpy)]PF_6$ [**PC1**; $E_{1/2}$ (*P/P$^-$), 1.21 V vs SCE; $E_{1/2}$ (P/P$^-$), −1.37 V vs SCE] and 4CzIPN [**PC6**; $E_{1/2}$ (*P/P$^-$), 1.35 V vs SCE; $E_{1/2}$ (P/P$^-$), −1.21 V vs SCE][16] afforded the target 1,3,3-trimethylindolin-2-one (**2a**) in 80% (entry 1) and 45% yields (entry 3), respectively. As a comparison, among others, $Ru(bpy)_3Cl_2$ (**PC2**), fac-$Ir(ppy)_3$ (**PC3**), Rose Bengal (**PC4**), and Eosin Y (**PC5**) only generated the 3,4-dihydroquinolinone product (entry 2). The strong Brønsted acid TfOH as a proton source was also critical to the chemoselectivity. Other acids tested gave no more than 20% yield of **2a** with poor chemoselectivity (entries 5 and 6), where a majority of **1a** was recovered with hydrobromination product generally formed in small amounts. The 5-exo-trig cyclization

Table 1. Screening Reaction Conditions[a]

entry	variation from standard conditions	yield (%)[b]
1	no variation	80
2	**PC2**−**PC5** instead of **PC1**	ND (5−20%)
3	**PC6** instead of **PC1**	45
4	no TfOH	ND
5	TFA or $Et_2O{\cdot}BF_3$ instead of TfOH	10, 20
6	AcOH or H_3PO_4 instead of TfOH	<5
7	no LiBr	19
8	TBAB, NaBr, or LiCl instead of LiBr	52, 57, 31
9	DCE, toluene, or MeOH as solvent	60, 66, 47
10	no H_2O	32
11	no light or no **PC1**	ND
12	under air	44

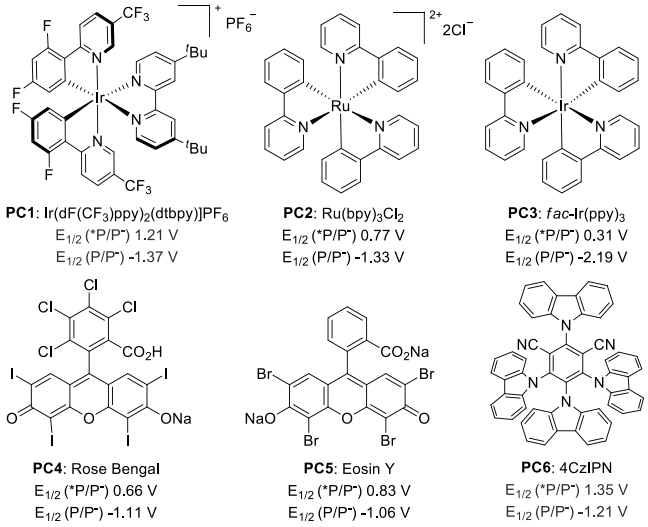

[a]The reaction was performed with **1a** (0.2 mmol), photocatalyst (**PC**, 2.0 mol %), TfOH (1.0 equiv), LiBr (30 mol %), H_2O (20 equiv), and PhCl (0.2 M) under a N_2 atmosphere with 35 W blue LEDs at room temperature (25−35 °C) for 24 h. [b]Isolated yields of **2a** were given. The yield of **3a** was determined by GC analysis using dodecane as an internal standard and was given in parentheses.

product was not formed in the absence of TfOH (entry 4). The yield in the absence of LiBr was dramatically declined to 19% (entry 7), and the majority of **1a** was recovered. Among others, TBAB, NaBr, and LiCl as additives were all given moderate productivities (entry 8). Some white solid remained during the reaction when it was performed without H_2O, which indicates that the role of H_2O is to enhance the solubility of the inorganic Brønsted acid and bromide additive (entry 9). Finally, the results of control experiments suggest that light stimulation, a photocatalyst, and an inert reaction atmosphere are all essential (entries 11 and 12), which rules out the hydroarylation process via the Friedel−Crafts carbocation mechanism. Notably, the 3,4-dihydroquinolinone product **3a** was not formed in all cases using **PC1** as the photocatalyst.

We initially probed the substrate scope (Figure 2) of the visible-light-induced intramolecular hydroarylation with various subsituents on the benzene ring of aniline moiety (R^1).

https://doi.org/10.1021/acscatal.1c00649
ACS Catal. 2021, 11, 4422−4429

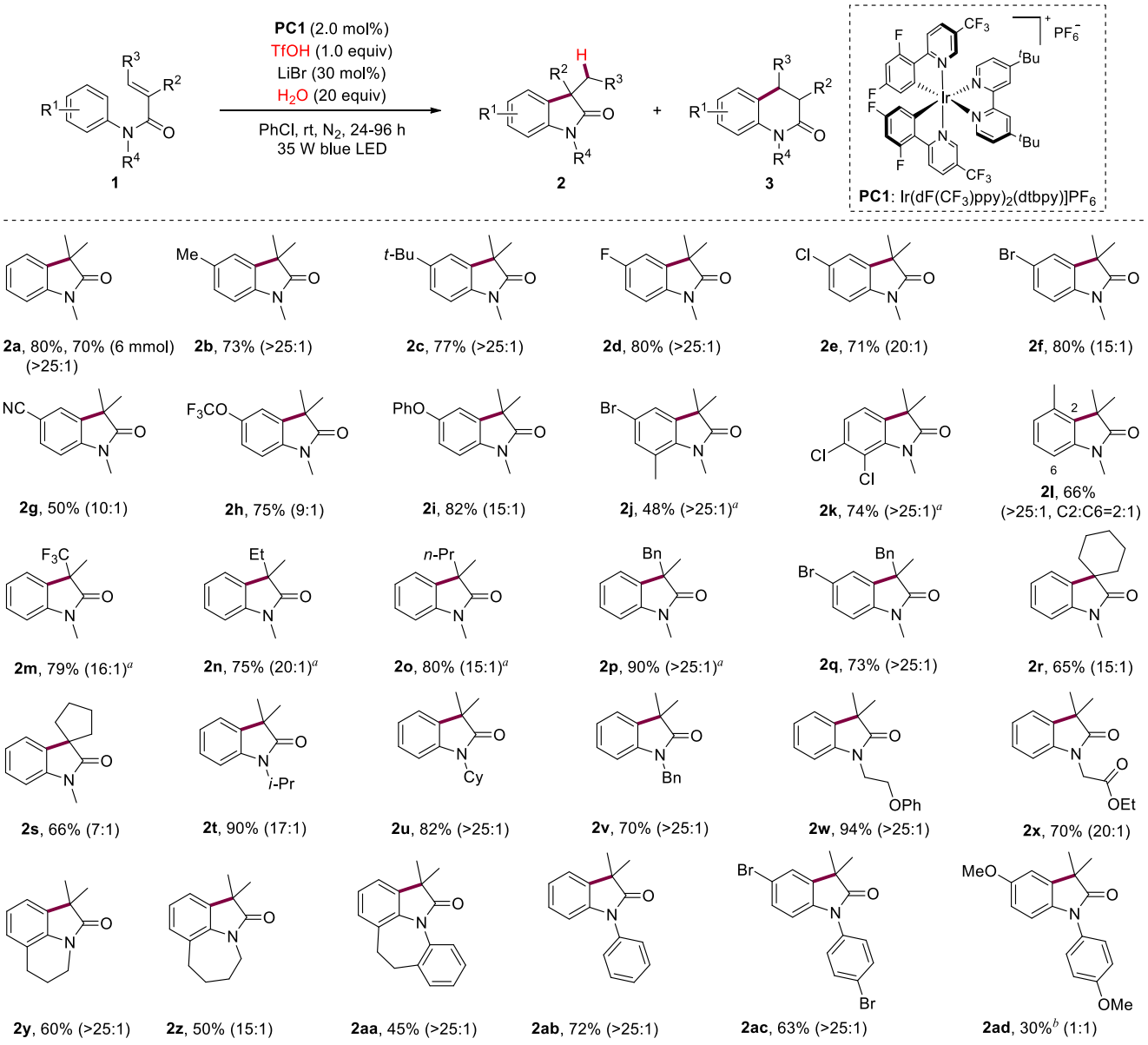

Figure 2. Substrate scope of the photochemical hydroarylation reactions (major products and combinational yields were given and the ratio of product **2** and **3** in parentheses was determined by GC analysis; [a]within 96 h; [b]yield of **2ad**).

Alkyl functionalities such as methyl (**2b**) and *tert*-butyl (**2c**) slightly declined the yields to 73% and 77%, respectively. Synthetically useful halogens including F, Cl, and Br were well tolerated to afford the corresponding halo oxindoles (**2d**−**2f**) in good yields (71−80% yields). While the electron-withdrawing cyano group gave only a moderate yield of product **2g** (50% yield), the substrates bearing trifluoromethoxy (**2h**, 75% yield) and phenoxy (**2i**, 82% yield) cyclized with excellent productivities. As a comparison, ortho-substituted reactants reduced the efficiency of the desired hydroarylation reaction (**2j**, 48% yield, and **2k**, 74% yield, respectively), in which the reactants were not consumed even within 96 h. Expectedly, the substrate with a meta substituent generated a mixture of two isomer cyclization products with minimal control over regioselectivity (**2l**, 66% yield, rr = 2:1). We also explored the generality of changing the *N*-methyl-*N*-phenylacrylamides via diversification of the N-acyl fragment of the molecule. The acrylamide with the α-trifluoromethyl group transferred completely with prolonged reaction time (79% yield). Other alkyls such as ethyl and propyl were also compatible, cyclizing in good yields (**2n**, 75% yield and **2o**, 80% yield). Introducing benzyl substituents in the α-position did not have obviously deleterious effects on the reaction (**2p**, 90% yield, and **2q**, 73% yield). Cyclic alkenes, i.e., therein, an alkyl substituent was added at the terminal end of the alkene, worked smoothly, leading to the formation of structurally important spiro oxindoles (**2r**, 65% yield, and **2s**, 66% yield). Regarding the functional group attached at the N atom, while free *N*-phenylacrylamide featured very low reactivity, higher yields were achieved when the bulky iso-propyl and cyclohexyl were incorporated (**2t**, 90% yield and **2u**, 82% yield, respectively). The benzyl protecting group was well tolerated to give **2v** in 70% yield, which could transfer into NH oxindoles via debenzylation. To our delight, the phenyl ether substrate cyclized with almost quantitative yield (**2w**, 94% yield). The glycine-derived *N*-phenylacrylamide also reacted with the compatible ester group in moderate yield (**2x**, 70% yield). Then, cyclic and diaryl N-acylamines were exploited to

https://doi.org/10.1021/acscatal.1c00649
ACS Catal. 2021, 11, 4422−4429

smoothly produce polycyclic products (**2y**−**2aa**) and N-aryl oxindoles (**2aa**−**2ad**) with yields ranging from 30% to 72%. The robust synthetic capability of our photochemical system for hydroarylation was further mirrored by the effective gram-scale production of oxindoles (70% yield of **2a** on 7 mmol scale). Notably, with the oxindole major products, the hydroarylation/cyclization also leads to the formation of 3,4-dihydroquinolinone in many cases of substrate scope. Moreover, the π-extension substrates such as 2-phenylacrylic amides (R^2 = Ph) and cinnamamides (R^3 = Ph) led to the formation of 3,4-dihydroquinolinones as the major products because of the superior electrocyclization reactivity.

Then, the reaction systems were found to tolerate the substrates attached with some drug molecules including ibuprofen (**2ae**), naproxen (**2af**), salicylic acid (**2ag**), and estrone (**2ah**), with yields ranging from 48% to 80% (Figure 3, top). From commercially available Tiglic acid and *N*-methylaniline, acrylamide **1ai** was conveniently prepared that cyclized to form oxindole **2ai** in 80% yield under our standard conditions. Further bromination and subsequent Suzuki−Miyaura coupling afforded the oxindole product **2ak**, a progesterone receptor antagonist[17] (Figure 3, middle). Moreover, hydroxyl acrylamide **1al**, derived from simple α-methylene-γ-butyrolactone, underwent intramolecular hydroarylation to furnish synthetically important hydroxyl oxindole **2al**. For example, it was readily transformed into formyl oxindole **2am**, a precursor compound of bioactive esermethole and physostigmine[18] using as a reversible inhibitor of acetylcholinesterase used for the treatment of glaucoma and Alzheimer's diseases. Alternatively, reductive cyclization of **2al** gave furo[2,3-*b*]indoline **2an**, which can further deliver physovenine via late-stage modification[19] (Figure 3, bottom).

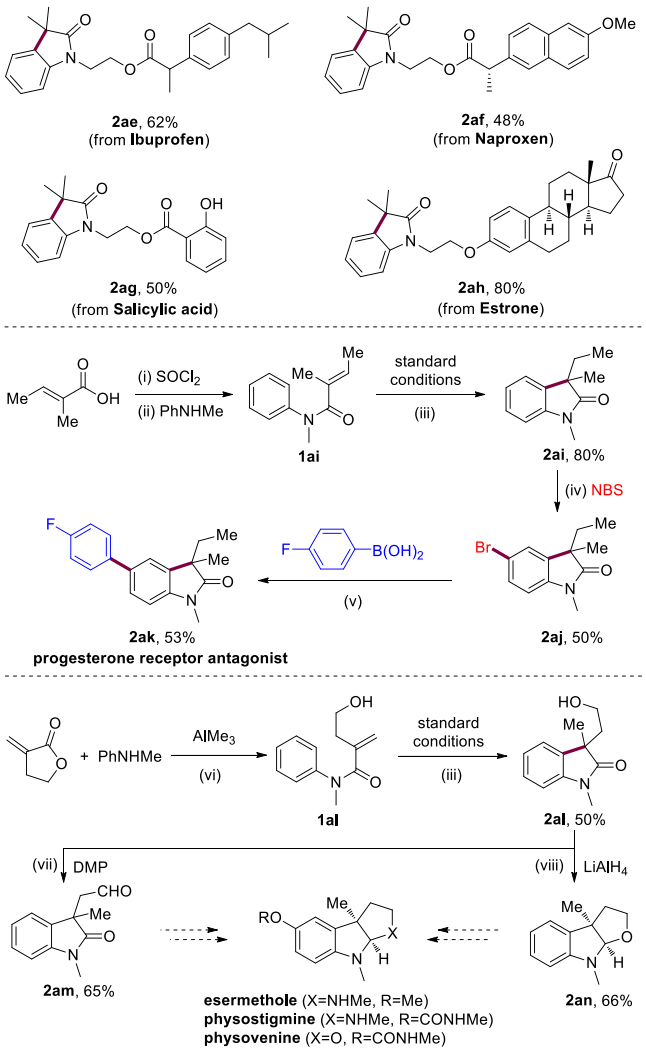

Figure 3. Application of the photochemical hydroarylation reaction.

While our **PC1**/TfOH/LiBr catalytic system enabled exclusive 5-exo-trig selectivity for all of the above reactants, N-(4-methoxyphenyl)-*N*-methylmethacrylamide (**1ao**) afforded oxindole **2ao** as the major product along with formation of the dihydroquinolinone product **3ao** via 6-endo-trig cyclization under the standard reaction conditions (76% yield, rr = 7.1:1). Notably, the ratio of **3ao** was enhanced in the absence of the LiBr additive (rr = 4.5:1), and the formation of **2ao** was completely suppressed when bromide and acid were both removed (Figure 4a). The results of cyano and chloro substrates in the absence of LiBr and TfOH (**2e**, **2g**) were also similar to those of **1ao** (see SI for details). Moreover, with the **PC1** and visible light treatment, the naphthylamine substrate proceeded exclusively via 6-endo-trig cyclization to afford benzodihydroquinolinone **3ap** in good yields even with bromide and acid additive (Figure 4b). These results can be attributed to the competitive electron transfer of bromide and energy transfer of substrates with the excited Ir complex. The Stern−Volmer quenching experiments indicate that LiBr quenched apparently the fluorescence emission of **PC1** (K_{SV}

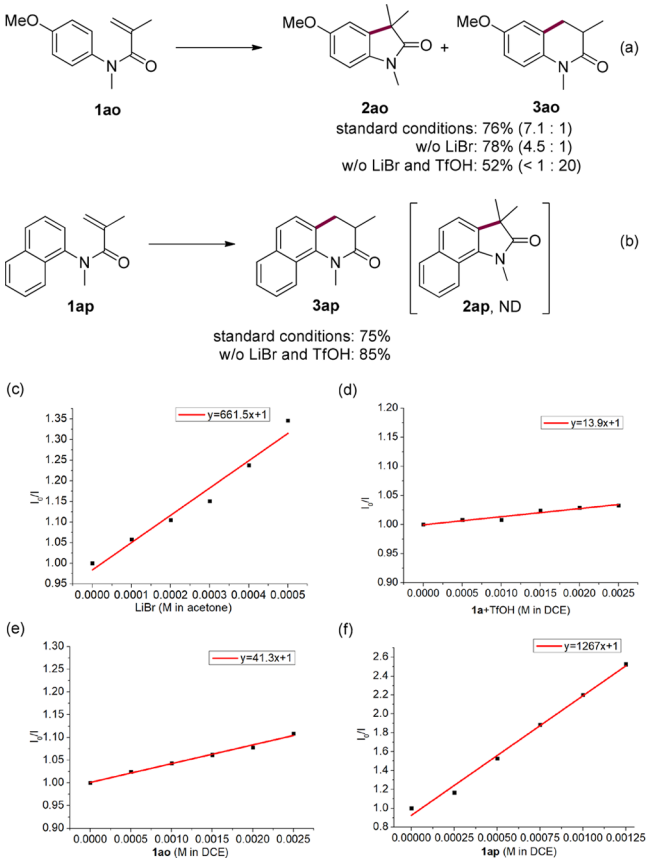

Figure 4. Formation of benzodihydroquinolinones and Stern−Volmer quenching experiments.

https://doi.org/10.1021/acscatal.1c00649
ACS Catal. 2021, 11, 4422−4429

= 661, Figure 4c), while normal substrates such as **1a** did not feature such an effect (Figure 4d). Mechanistically, the bromide additive may serve as the initial reductive quencher [$E_{1/2}^{red}$ ($Br^{\bullet}/Br^{-}$), 0.80 V vs SCE in dimethoxyethane][20] to the excited iridium(III) complex [***PC1**; $E_{1/2}$ (*P/P^{-}), 1.21 V] to generate iridium(II) with high reductive potential [$E_{1/2}$ (P/P^{-}), −1.37 V]. In the case of **1ao**, however, the fluorescence quenching effect by energy transfer from ***PC1** was observed (K_{SV} = 41, Figure 4e) that led to considerable formation of dihydroquinolinone product. The naphthylamine substrate exhibited the most quenching effect (K_{SV} = 1267, Figure 4f), which resulted in absolutely advantaged energy transfer to generate the 6-endo-trig cyclization product.

The H/D exchange experiments show that no D incorporation of the cyclized product was observed when D5-labeled N-acylaniline (D_5-**1a**) was employed (Figure 5a)

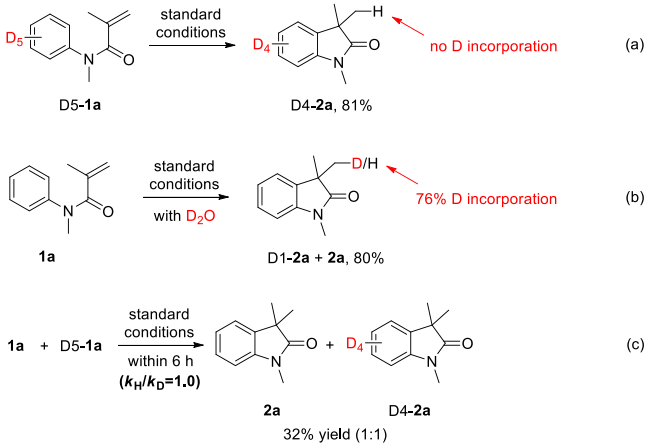

Figure 5. H/D exchange and KIE experiments.

and the addition of D_2O led to 76% D incorporation in the newly formed methyl group (Figure 5b), indicating a PCET process in the initial step. The competitive kinetic experiments with **1a** and D_5-**1a** under the standard conditions determined a kinetic isotopic effect (KIE) of k_H/k_D = 1.0 (Figure 5c), thus revealing the C−H scission of the aniline moiety to occur after the rate-determining step.

During the studies on optimizing reaction conditions, we observed the photochemical formation of α-bromoamide **4a**, which could be enhanced by the addition of stoichiometric LiBr within reduced reaction time (Figure 6a). This kind of compound could transform into the final cyclized product **2a** under previously reported photocatalytic systems[21] as well as our standard conditions (Figure 6b). In comparison, while the N-methophenyl α-bromoamide **4b** afforded only 5-exo-trig cyclization product **2ao** (Figure 6c), the naphthyl variant **5c** furnished a mixture of benzoxindole **2ap** and benzodihydroquinolinone **3ap** (Figure 6d). These results suggest a reversible radical bromination process. While the results of radical trap experiments also revealed a radical mechanism, the light-on/off experiments rule out a free radical chain pathway (see SI).

While hydroarylation reaction via 6π-electrocyclization under photoirradiation has been well established, based on the above experimental results, we proposed a tentative reaction mechanism of our intramolecular hydroarylation reaction with 5-exo-trig selectivity (Figure 7). Initially, the photosensitizer Ir^{III} complex (**PC1**) absorbs photons to form highly oxidative $*Ir^{III}$, which is reduced by the bromide anion

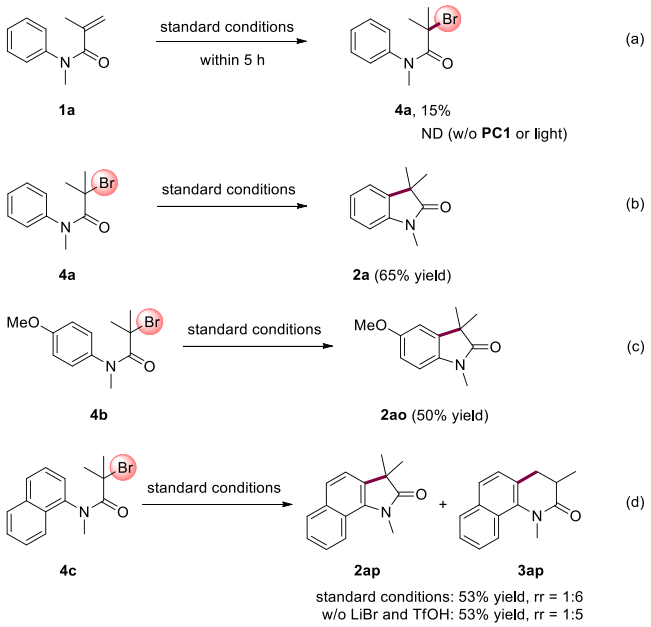

Figure 6. Productivity of α-bromoamides.

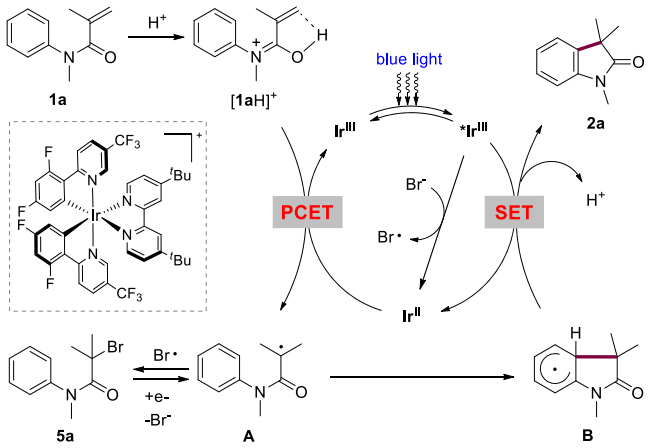

Figure 7. Possible reaction mechanism.

to give a highly reductive Ir^{II} species and a bromo radical.[22] Simultaneously, with the strong Brønsted acid treatment, **1a** was coupled with a proton to form a [**1a**H]$^+$ ion. Then, single electron transfer from Ir^{II} to [**1a**H]$^+$ generates the α-radical amide **A**,[23] which could couple with the bromo radical to produce the side product α-bromoamide **5a**. In that case, **5a** could also decompose to **A** by reductive bromo elimination. Subsequently, radical cyclization of **A** occurs to deliver intermediate **B**.[14] Finally, **B** is oxidized by the highly oxidative $*Ir^{III}$ complex followed by deprotonation to produce the oxindole product **2a**.

In summary, we have developed a mild visible-light-induced photoredox neutral hydroarylation reaction of N-arylacrylamides for the synthesis of oxindoles. The present protocol provides a straightforward and mild entry to pharmaceutically important oxindoles with a broad range of compatible functionalities. Beyond the well established photoinduced 6π electrocyclization of this reactant, the present photocatalytic system combined with Brønsted acid and bromide additive features high 5-exo-trig selectivity through proton-coupled electron transfer (PCET). LiBr proved to be critical in such a

https://doi.org/10.1021/acscatal.1c00649
ACS Catal. 2021, 11, 4422−4429

PCET process that probably reduces the excited photocatalyst to form highly reductive Ir^{II} species. The novel photoredox system enables the PCET process of electron-deficient alkenes that may have broad applications in hydrofunctionalization reactions of alkenes, although it still faces the scope issues raised from the strong acidic conditions.

■ ASSOCIATED CONTENT

Supporting Information

The Supporting Information is available free of charge at https://pubs.acs.org/doi/10.1021/acscatal.1c00649.

Experimental procedures, detailed mechanistic studies, characterization data, and ^{1}H NMR and ^{13}C NMR spectra for all new products (PDF)

■ AUTHOR INFORMATION

Corresponding Authors

Xiaochen Ji − *Key Laboratory for Green Organic Synthesis and Application of Hunan Province, Key Laboratory of Environmentally Friendly Chemistry and Application of Ministry of Education, College of Chemistry, Xiangtan University, Xiangtan 411105, China*; Email: xcji@xtu.edu.cn

Huawen Huang − *Key Laboratory for Green Organic Synthesis and Application of Hunan Province, Key Laboratory of Environmentally Friendly Chemistry and Application of Ministry of Education, College of Chemistry, Xiangtan University, Xiangtan 411105, China*; orcid.org/0000-0001-7079-1299; Email: hwhuang@xtu.edu.cn

Authors

Zhaosheng Liu − *Key Laboratory for Green Organic Synthesis and Application of Hunan Province, Key Laboratory of Environmentally Friendly Chemistry and Application of Ministry of Education, College of Chemistry, Xiangtan University, Xiangtan 411105, China*

Shuai Zhong − *Key Laboratory for Green Organic Synthesis and Application of Hunan Province, Key Laboratory of Environmentally Friendly Chemistry and Application of Ministry of Education, College of Chemistry, Xiangtan University, Xiangtan 411105, China*

Guo-Jun Deng − *Key Laboratory for Green Organic Synthesis and Application of Hunan Province, Key Laboratory of Environmentally Friendly Chemistry and Application of Ministry of Education, College of Chemistry, Xiangtan University, Xiangtan 411105, China*; orcid.org/0000-0003-2759-0314

Complete contact information is available at: https://pubs.acs.org/10.1021/acscatal.1c00649

Notes

The authors declare no competing financial interest.

■ ACKNOWLEDGMENTS

Financial support by the National Natural Science Foundation of China (22071211, 21502161), the Science and Technology Planning Project of Hunan Province (2019RS2039), Hunan Provincial Natural Science Foundation of China (2020JJ3032), Scientific Research Fund of Education Department of Hunan Province (18C0089), and the Collaborative Innovation Center of New Chemical Technologies for Environmental Benignity and Efficient Resource Utilization is gratefully acknowledged.

■ REFERENCES

(1) (a) Crossley, S. W.; Obradors, C.; Martinez, R. M.; Shenvi, R. A. Mn-, Fe-, and Co-Catalyzed Radical Hydrofunctionalizations of Olefins. *Chem. Rev.* **2016**, *116*, 8912−9000. (b) Jana, R.; Pathak, T. P.; Sigman, M. S. Advances in transition metal (Pd, Ni, Fe)-catalyzed cross-coupling reactions using alkyl-organometallics as reaction partners. *Chem. Rev.* **2011**, *111*, 1417−1492. (c) Zeng, X. Recent advances in catalytic sequential reactions involving hydroelement addition to carbon-carbon multiple bonds. *Chem. Rev.* **2013**, *113*, 6864−6900. (d) Blieck, R.; Taillefer, M.; Monnier, F. Metal-Catalyzed Intermolecular Hydrofunctionalization of Allenes: Easy Access to Allylic Structures via the Selective Formation of C-N, C-C, and C-O Bonds. *Chem. Rev.* **2020**, *120*, 13545−13598.

(2) (a) Biffis, A.; Centomo, P.; Del Zotto, A.; Zecca, M. Pd Metal Catalysts for Cross-Couplings and Related Reactions in the 21st Century: A Critical Review. *Chem. Rev.* **2018**, *118*, 2249−2295. (b) Le Bras, J.; Muzart, J. Intermolecular dehydrogenative Heck reactions. *Chem. Rev.* **2011**, *111*, 1170−1214. (c) Gandeepan, P.; Muller, T.; Zell, D.; Cera, G.; Warratz, S.; Ackermann, L. 3d Transition Metals for C-H Activation. *Chem. Rev.* **2019**, *119*, 2192−2452.

(3) (a) Gui, Q.; Hu, L.; Chen, X.; Liu, J.; Tan, Z. Synthesis of Oxindoles via Iron-Mediated Hydrometallation-Cyclization of N-Arylacrylamides. *Asian J. Org. Chem.* **2015**, *4*, 870−874. (b) Kilaru, P.; Acharya, S. P.; Zhao, P. A tethering directing group strategy for ruthenium-catalyzed intramolecular alkene hydroarylation. *Chem. Commun.* **2018**, *54*, 924−927. (c) Lu, K.; Han, X.-W.; Yao, W.-W.; Luan, Y.-X.; Wang, Y.-X.; Chen, H.; Xu, X.-T.; Zhang, K.; Ye, M. DMF-Promoted Redox-Neutral Ni-Catalyzed Intramolecular Hydroarylation of Alkene with Simple Arene. *ACS Catal.* **2018**, *8*, 3913−3917. (d) Liu, W.; Ackermann, L. Manganese-Catalyzed C−H Activation. *ACS Catal.* **2016**, *6*, 3743−3752. (e) Carral-Menoyo, A.; Sotomayor, N.; Lete, E. Cp*Co(III)-Catalyzed C-H Hydroarylation of Alkynes and Alkenes and Beyond: A Versatile Synthetic Tool. *ACS omega* **2020**, *5*, 24974−24993. (f) Kyne, S. H.; Lefevre, G.; Ollivier, C.; Petit, M.; Ramis Cladera, V. A.; Fensterbank, L. Iron and cobalt catalysis: new perspectives in synthetic radical chemistry. *Chem. Soc. Rev.* **2020**, *49*, 8501−8542.

(4) (a) Gansauer, A.; Behlendorf, M.; von Laufenberg, D.; Fleckhaus, A.; Kube, C.; Sadasivam, D. V.; Flowers, R. A., II Catalytic, atom-economical radical arylation of epoxides. *Angew. Chem., Int. Ed.* **2012**, *51*, 4739−4742. (b) Gansauer, A.; von Laufenberg, D.; Kube, C.; Dahmen, T.; Michelmann, A.; Behlendorf, M.; Sure, R.; Seddiqzai, M.; Grimme, S.; Sadasivam, D. V.; Fianu, G. D.; Flowers, R. A., II 2nd Mechanistic study of the titanocene(III)-catalyzed radical arylation of epoxides. *Chem. - Eur. J.* **2015**, *21*, 280−289. (c) Muhlhaus, F.; Weissbarth, H.; Dahmen, T.; Schnakenburg, G.; Gansauer, A. Merging Regiodivergent Catalysis with Atom-Economical Radical Arylation. *Angew. Chem., Int. Ed.* **2019**, *58*, 14208−14212.

(5) (a) Xuan, J.; Xiao, W. J. Visible-light photoredox catalysis. *Angew. Chem., Int. Ed.* **2012**, *51*, 6828−6838. (b) Prier, C. K.; Rankic, D. A.; MacMillan, D. W. Visible light photoredox catalysis with transition metal complexes: applications in organic synthesis. *Chem. Rev.* **2013**, *113*, 5322−5363. (c) Skubi, K. L.; Blum, T. R.; Yoon, T. P. Dual Catalysis Strategies in Photochemical Synthesis. *Chem. Rev.* **2016**, *116*, 10035−10074. (d) Narayanam, J. M.; Stephenson, C. R. Visible light photoredox catalysis: applications in organic synthesis. *Chem. Soc. Rev.* **2011**, *40*, 102−113. (e) Ravelli, D.; Dondi, D.; Fagnoni, M.; Albini, A. Photocatalysis. A multi-faceted concept for green chemistry. *Chem. Soc. Rev.* **2009**, *38*, 1999−2011. (f) Yoon, T. P.; Ischay, M. A.; Du, J. Visible light photocatalysis as a greener approach to photochemical synthesis. *Nat. Chem.* **2010**, *2*, 527−532. (g) Schultz, D. M.; Yoon, T. P. Solar synthesis: prospects in visible light photocatalysis. *Science* **2014**, *343*, 1239176.

(6) (a) Ramamurthy, V.; Sivaguru, J. Supramolecular Photochemistry as a Potential Synthetic Tool: Photocycloaddition. *Chem. Rev.* **2016**, *116*, 9914−9993. (b) Poplata, S.; Troster, A.; Zou, Y. Q.; Bach, T. Recent Advances in the Synthesis of Cyclobutanes by Olefin

[2 + 2] Photocycloaddition Reactions. *Chem. Rev.* **2016**, *116*, 9748−9815.
(7) (a) Cleveland, P. G.; Chapman, O. L. Non-oxidative Photocyclizations of Alkyl-substituted Acrylic Acid Anilides to Dihydrocarbostyrils. *Chem. Commun.* **1967**, *3*, 1064−1065. (b) Jia, J.; Sarker, M.; Steinmetz, M. G.; Shukla, R.; Rathore, R. Photochemical Elimination of Leaving Groups from Zwitterionic Intermediates Generated via Electrocyclic Ring Closure of α,β-Unsaturated Anilides. *J. Org. Chem.* **2008**, *73*, 8867−8879. (c) Ayitou, A. J.; Ugrinov, A.; Sivaguru, J. 6π-Photocyclization of O-tert-butylacrylanilides. N-substitution dictates the regiochemistry of cyclization. *Photochem. Photobiol. Sci.* **2009**, *8*, 751−754. (d) Ayitou, A. J.; Sivaguru, J. Reactive spin state dependent enantiospecific photocyclization of axially chiral alpha-substituted acrylanilides. *Chem. Commun.* **2011**, *47*, 2568−2570. (e) Ayitou, A. J.; Vallavoju, N.; Ugrinov, A.; Sivaguru, J. Enantiospecific 6pi-photocyclization of atropisomeric alpha-substituted acrylanilides in the solid-state: role of crystalline confinement on enantiospecificity. *Photochem. Photobiol. Sci.* **2011**, *10*, 1380−1383. (f) Raghunathan, R.; Jockusch, S.; Sibi, M. P.; Sivaguru, J. Evaluating thiourea/urea catalyst for enantioselective 6π-photocyclization of acrylanilides. *J. Photochem. Photobiol., A* **2016**, *331*, 84−88. (g) Li, L.; Ndzeidze, G. N.; Steinmetz, M. G. Photochemical electrocyclization and leaving group expulsion with a naphthothiophene-2-carboxanilide linked to a chromophore. *Tetrahedron* **2019**, *75*, 70−83.
(8) (a) Ischay, M. A.; Anzovino, M. E.; Du, J.; Yoon, T. P. Efficient Visible Light Photocatalysis of [2 + 2] Enone Cycloadditions. *J. Am. Chem. Soc.* **2008**, *130*, 12886−12887. (b) Yoon, T. P. Visible Light Photocatalysis: The Development of Photocatalytic Radical Ion Cycloadditions. *ACS Catal.* **2013**, *3*, 895−902. (c) Du, J.; Skubi, K. L.; Schultz, D. M.; Yoon, T. P. A Dual-Catalysis Approach to Enantioselective [2 + 2] Photocycloadditions Using Visible Light. *Science* **2014**, *344*, 392−396. (d) Liu, Y.; Song, R.; Li, J. The cycloaddition reaction using visible light photoredox catalysis. *Sci. China: Chem.* **2016**, *59*, 161−170. (e) Nakashima, T.; Tsuchie, K.; Kanazawa, R.; Li, R.; Iijima, S.; Galangau, O.; Nakagawa, H.; Mutoh, K.; Kobayashi, Y.; Abe, J.; Kawai, T. Self-Contained Photoacid Generator Triggered by Photocyclization of Triangle Terarylene Backbone. *J. Am. Chem. Soc.* **2015**, *137*, 7023−7026. (f) Chen, Y.; Lu, L.-Q.; Yu, D.-G.; Zhu, C.-J.; Xiao, W.-J. Visible light-driven organic photochemical synthesis in China. *Sci. China: Chem.* **2019**, *62*, 24−57.
(9) Popescu, M. V.; Mekereeya, A.; Alegre-Requena, J. V.; Paton, R. S.; Smith, M. Visible-Light-Mediated Heterocycle Functionalization via Geometrically Interrupted [2 + 2] Cycloaddition. *Angew. Chem., Int. Ed.* **2020**, *59*, 23020−23024.
(10) Cheng, H.; Lam, T.-L.; Liu, Y.; Tang, Z.; Che, C.-M. Photoinduced Hydroarylation and Cyclization of Alkenes with Luminescent Platinum(II) Complexes. *Angew. Chem., Int. Ed.* **2021**, *60*, 1383−1389.
(11) (a) Gentry, E. C.; Knowles, R. R. Synthetic Applications of Proton-Coupled Electron Transfer. *Acc. Chem. Res.* **2016**, *49*, 1546−1556. (b) Hoffmann, N. Proton-Coupled Electron Transfer in Photoredox Catalytic Reactions. *Eur. J. Org. Chem.* **2017**, *2017*, 1982−1992. (c) Yang, J. D.; Ji, P.; Xue, X. S.; Cheng, J. P. Recent Advances and Advisable Applications of Bond Energetics in Organic Chemistry. *J. Am. Chem. Soc.* **2018**, *140*, 8611−8623. (d) Xia, Q.; Dong, J.; Song, H.; Wang, Q. Visible-Light Photocatalysis of the Ketyl Radical Coupling Reaction. *Chem.—Eur. J.* **2019**, *25*, 2949−2961.
(12) (a) Rono, L. J.; Yayla, H. G.; Wang, D. Y.; Armstrong, M. F.; Knowles, R. R. Enantioselective photoredox catalysis enabled by proton-coupled electron transfer: development of an asymmetric aza-pinacol cyclization. *J. Am. Chem. Soc.* **2013**, *135*, 17735−17738. (b) Tarantino, K. T.; Liu, P.; Knowles, R. R. Catalytic ketyl-olefin cyclizations enabled by proton-coupled electron transfer. *J. Am. Chem. Soc.* **2013**, *135*, 10022−10025. (c) Lee, K. N.; Lei, Z.; Ngai, M. Y. beta-Selective Reductive Coupling of Alkenylpyridines with Aldehydes and Imines via Synergistic Lewis Acid/Photoredox Catalysis. *J. Am. Chem. Soc.* **2017**, *139*, 5003−5006. (d) Pitzer, L.; Sandfort, F.; Strieth-Kalthoff, F.; Glorius, F. Intermolecular Radical Addition to Carbonyls Enabled by Visible Light Photoredox Initiated Hole Catalysis. *J. Am. Chem. Soc.* **2017**, *139*, 13652−13655. (e) Rossolini, T.; Leitch, J. A.; Grainger, R.; Dixon, D. J. Photocatalytic Three-Component Umpolung Synthesis of 1,3-Diamines. *Org. Lett.* **2018**, *20*, 6794−6798. (f) Cao, K.; Tan, S. M.; Lee, R.; Yang, S.; Jia, H.; Zhao, X.; Qiao, B.; Jiang, Z. Catalytic Enantioselective Addition of Prochiral Radicals to Vinylpyridines. *J. Am. Chem. Soc.* **2019**, *141*, 5437−5443. (g) Qiu, G.; Knowles, R. R. Rate-Driving Force Relationships in the Multisite Proton-Coupled Electron Transfer Activation of Ketones. *J. Am. Chem. Soc.* **2019**, *141*, 2721−2730.
(13) (a) Betori, R. C.; McDonald, B. R.; Scheidt, K. A. Reductive annulations of arylidene malonates with unsaturated electrophiles using photoredox/Lewis acid cooperative catalysis. *Chem. Sci.* **2019**, *10*, 3353−3359. (b) Betori, R. C.; Scheidt, K. A. Reductive Arylation of Arylidene Malonates Using Photoredox Catalysis. *ACS Catal.* **2019**, *9*, 10350−10357.
(14) Li, J.-H.; Song, R.-J.; Liu, Y.; Xie, Y.-X. Difunctionalization of Acrylamides through C−H Oxidative Radical Coupling: New Approaches to Oxindoles. *Synthesis* **2015**, *47*, 1195−1209.
(15) (a) Wu, T.; Mu, X.; Liu, G. Palladium-catalyzed oxidative arylalkylation of activated alkenes: dual C-H bond cleavage of an arene and acetonitrile. *Angew. Chem., Int. Ed.* **2011**, *50*, 12578−12581. (b) Mu, X.; Wu, T.; Wang, H. Y.; Guo, Y. L.; Liu, G. Palladium-catalyzed oxidative aryltrifluoromethylation of activated alkenes at room temperature. *J. Am. Chem. Soc.* **2012**, *134*, 878−881. (c) Wei, W. T.; Zhou, M. B.; Fan, J. H.; Liu, W.; Song, R. J.; Liu, Y.; Hu, M.; Xie, P.; Li, J. H. Synthesis of oxindoles by iron-catalyzed oxidative 1,2-alkylarylation of activated alkenes with an aryl C(sp2)-H bond and a C(sp3)-H bond adjacent to a heteroatom. *Angew. Chem., Int. Ed.* **2013**, *52*, 3638−3641. (d) Fan, J. H.; Wei, W. T.; Zhou, M. B.; Song, R. J.; Li, J. H. Palladium-catalyzed oxidative difunctionalization of alkenes with alpha-carbonyl alkyl bromides initiated through a Heck-type insertion: a route to indolin-2-ones. *Angew. Chem., Int. Ed.* **2014**, *53*, 6650−6654. (e) Theunissen, C.; Wang, J.; Evano, G. Copper-catalyzed direct alkylation of heteroarenes. *Chem. Sci.* **2017**, *8*, 3465−3470. (f) Ratushnyy, M.; Kvasovs, N.; Sarkar, S.; Gevorgyan, V. Visible-Light-Induced Palladium-Catalyzed Generation of Aryl Radicals from Aryl Triflates. *Angew. Chem., Int. Ed.* **2020**, *59*, 10316−10320.
(16) Luo, J.; Zhang, J. Donor−Acceptor Fluorophores for Visible-Light-Promoted Organic Synthesis: Photoredox/Ni Dual Catalytic C(sp3)−C(sp2) Cross-Coupling. *ACS Catal.* **2016**, *6*, 873−877.
(17) Alluri, S.; Feng, H.; Livings, M.; Samp, L.; Biswas, D.; Lam, T. W.; Lobkovsky, E.; Ganguly, A. K. A convenient enantioselective synthesis of 3-asymmetrically substituted oxindoles as progesterone receptor antagonists. *Tetrahedron Lett.* **2011**, *52*, 3945−3948.
(18) Kong, W.; Wang, Q.; Zhu, J. Palladium-Catalyzed Enantioselective Domino Heck/Intermolecular C-H Bond Functionalization: Development and Application to the Synthesis of (+)-Esermethole. *J. Am. Chem. Soc.* **2015**, *137*, 16028−16031.
(19) Kulkarni, M. G.; Dhondge, A. P.; Borhade, A. S.; Gaikwad, D. D.; Chavhan, S. W.; Shaikh, Y. B.; Nigdale, V. B.; Desai, M. P.; Birhade, D. R.; Shinde, M. P. Total Synthesis of (±)-Physovenine. *Eur. J. Org. Chem.* **2009**, *2009*, 3875−3877.
(20) Zhang, P.; Le, C. C.; MacMillan, D. W. Silyl Radical Activation of Alkyl Halides in Metallaphotoredox Catalysis: A Unique Pathway for Cross-Electrophile Coupling. *J. Am. Chem. Soc.* **2016**, *138*, 8084−8087.
(21) Black, M. J.; Biegasiewicz, K. F.; Meichan, A. J.; Oblinsky, D. G.; Kudisch, B.; Scholes, G. D.; Hyster, T. K. Asymmetric redox-neutral radical cyclization catalysed by flavin-dependent 'ene'-reductases. *Nat. Chem.* **2020**, *12*, 71−75.
(22) (a) Wang, Z.; Liu, Q.; Ji, X.; Deng, G.-J.; Huang, H. Bromide-Promoted Visible-Light-Induced Reductive Minisci Reaction with Aldehydes. *ACS Catal.* **2020**, *10*, 154−159. (b) Wang, Z.; Ji, X.; Han, T.; Deng, G. J.; Huang, H. LiBr-Promoted Photoredox Minisci-Type Alkylations of Quinolines with Ethers. *Adv. Synth. Catal.* **2019**, *361*, 5643−5647. (c) Ji, X.; Liu, Q.; Wang, Z.; Wang, P.; Deng, G.-J.; Huang, H. LiBr-promoted photoredox neutral Minisci hydroxyalky-

https://doi.org/10.1021/acscatal.1c00649
ACS Catal. 2021, 11, 4422−4429

lations of quinolines with aldehydes. *Green Chem.* **2020**, *22*, 8233−8237. (d) Wang, Z.; Ji, X.; Zhao, J.; Huang, H. Visible-light-mediated photoredox decarbonylative Minisci-type alkylation with aldehydes under ambient air conditions. *Green Chem.* **2019**, *21*, 5512−5516. (e) Kawasaki, T.; Ishida, N.; Murakami, M. Dehydrogenative Coupling of Benzylic and Aldehydic C-H Bonds. *J. Am. Chem. Soc.* **2020**, *142*, 3366−3370.

(23) Sandoval, B. A.; Meichan, A. J.; Hyster, T. K. Enantioselective Hydrogen Atom Transfer: Discovery of Catalytic Promiscuity in Flavin-Dependent 'Ene'-Reductases. *J. Am. Chem. Soc.* **2017**, *139*, 11313−11316.

https://doi.org/10.1021/acscatal.1c00649
ACS Catal. 2021, 11, 4422−4429